

# Suppression of Choroidal Neovascularization by Vasohibin-1, a Vascular Endothelium-Derived Angiogenic Inhibitor

Ryosuke Wakusawa,<sup>1,2</sup> Toshiaki Abe,<sup>1</sup> Hajime Sato,<sup>2</sup> Hikaru Sonoda,<sup>3</sup> Masaaki Sato,<sup>3</sup> Yuuichi Mitsuda,<sup>3</sup> Tomoaki Takakura,<sup>3</sup> Tomi Fukushima,<sup>3</sup> Hideyuki Onami,<sup>1,2</sup> Nobuhiro Nagai,<sup>1</sup> Yumi Ishikawa,<sup>1</sup> Kohji Nishida,<sup>2</sup> and Yasufumi Sato<sup>4</sup>

**PURPOSE.** To determine the expression of vasohibin-1 during the development of experimentally induced choroidal neovascularization (CNV) and to investigate the effect of vasohibin-1 on the generation of CNV.

**METHODS.** CNV lesions were induced in the eyes of wild-type (WT) and vasohibin-1 knockout (KO) mice by laser photocoagulation. The expression of vasohibin-1, vascular endothelial growth factor (VEGF), VEGF receptor-1 (VEGFR1), VEGFR2, and pigment epithelial-derived factor (PEDF) was determined by semiquantitative reverse transcription-polymerase chain reaction. The expression of vasohibin-1 was also examined by immunohistochemistry with anti-CD68, anti- $\alpha$ SMA, anti-cytokeratin, and anti-CD31. Vasohibin-1 was injected into the vitreous and the activity and size of the CNV were determined by fluorescein angiography and in choroidal flat mounts.

**RESULTS.** Vasohibin-1 was detected not only in CD31-positive endothelial cells but also in CD68-positive macrophages and  $\alpha$ SMA-positive retinal pigment epithelial cells. Strong vasohibin-1 expression was observed at day 28, when the CNV lesions had regressed by histologic examination. The vasohibin-1 level was significantly decreased at day 14 and increased at day 28 after laser application. Significantly less VEGFR2 expression was observed on day 4 after vasohibin-1. The expression of PEDF was not significantly changed by vasohibin-1 injection. Vasohibin-1 injection significantly suppressed the CNV, with no adverse side effects. The CNV lesions in the vasohibin-1-KO mice were significantly larger than those in the WT mice.

**CONCLUSIONS.** The endogenous expression of vasohibin-1 is associated with the natural course of the development of CNV. Intravitreal injections of vasohibin-1 may be a method for inhibiting CNV. (*Invest Ophthalmol Vis Sci.* 2011;52:3272-3280) DOI:10.1167/iovs.10-6295

The most common cause of central vision loss in the elderly population of developed countries is age-related macular degeneration (AMD), and the cause of the vision loss in the exudative form of AMD is choroidal neovascularization (CNV).<sup>1</sup> CNV leads to subretinal hemorrhages, exudative lesions, serous retinal detachment, and disciform scars.<sup>2</sup>

Vascular endothelial cells (ECs), retinal pigment epithelial (RPE) cells, and macrophage-like mononuclear cells are the major cellular components of CNV membranes, and they produce many types of proangiogenic and antiangiogenic factors.<sup>3-10</sup> Vascular endothelial growth factor (VEGF), a proangiogenic factor, plays a major role in the development of CNV.<sup>11</sup>

Experimental studies have led to the development of anti-VEGF treatments for patients with AMD,<sup>10,12,13</sup> and such therapies are being successfully used. However, there are some disadvantages of VEGF therapy. First, monthly administration of anti-VEGF is necessary to maintain stable vision.<sup>14</sup> The repeated intravitreal injections are stressful for patients and doctors and can lead to irritation, infection, and other side effects.<sup>15</sup> Second, not all patients respond to VEGF therapy.<sup>16</sup> Third, anti-VEGF therapy blocks the antiapoptotic activity of VEGF, which is essential for the survival of the vascular ECs and nonvascular cells developmentally and in adults.<sup>17,18</sup> Indeed, VEGF is essential for the maintenance of the choriocapillaris and neural retina.<sup>19-21</sup> However, it is still being debated whether a prolonged blockade of VEGF will alter the systemic and ocular homeostasis.<sup>15,22,23</sup> Because of the adverse effects of anti-VEGF therapy, anti-VEGF antibody should be used with caution and other antiangiogenic agents should be considered.

Vasohibin-1 is a VEGF-inducible gene in human cultured ECs and has antiangiogenic properties.<sup>24,25</sup> The antiangiogenic properties were noted after it was shown that recombinant vasohibin-1 inhibited the network formation of ECs in vitro and also inhibited retinal neovascularization in a mouse model of oxygen-induced ischemic retinopathy.<sup>24,26</sup> Vasohibin-1 differs from other angiogenesis inhibitors by being selectively induced in ECs by proangiogenic factors such as VEGF and basic fibroblast growth factor (bFGF).<sup>24,27</sup> Thus, vasohibin-1 is considered to be an intrinsic and highly specific negative feedback regulator of activated ECs engaged in angiogenesis.

We recently found that vasohibin-1 is expressed in the CNV membranes obtained from human eyes with AMD.<sup>28</sup> Of note, eyes with lower ratios of vasohibin-1 to VEGF expression tended to have larger subretinal hemorrhages and vitreous hemorrhages,

From the <sup>1</sup>Division of Clinical Cell Therapy, Center for Advanced Medical Research and Development, the <sup>2</sup>Department of Ophthalmology and Visual Science, and the <sup>3</sup>Department of Vascular Biology, Institute of Development, Aging, and Cancer, Tohoku University Graduate School of Medicine, Miyagi, Japan; and the <sup>4</sup>Discovery Research Laboratories, Shionogi and Co. Ltd, Osaka, Japan.

Supported in part by Grants-in-Aid for Scientific Research 21592214 and 20592030 (TA) from the Japan Society for the Promotion of Science, Chiyoda-ku, Tokyo, Japan

Submitted for publication July 28, 2010; revised November 30, 2010, and January 28, 2011; accepted January 30, 2011.

Disclosure: R. Wakusawa, None; T. Abe, None; H. Sato, None; H. Sonoda, None; M. Sato, None; Y. Mitsuda, None; T. Takakura, None; T. Fukushima, None; H. Onami, None; N. Nagai, None; Y. Ishikawa, None; K. Nishida, None; Y. Sato, None

Corresponding author: Toshiaki Abe, Division of Clinical Cell Therapy, United Center for Advanced Research and Translational Medicine (ART), Tohoku University, Graduate School of Medicine, 1-1 Seiryomachi Aobaku Sendai, Miyagi, 980-8574 Japan; toshi@oph.med.tohoku.ac.jp.

whereas eyes with a higher vasohibin-1/VEGF ratio had subretinal fibrosis-like lesions.

The purpose of this study was to examine the vasohibin-1 expression during the development of experimentally induced CNV and to investigate the effect of vasohibin-1 on the generation of a CNV. To accomplish this, we first examined the expression of vasohibin-1 during the course of laser-induced CNV and evaluated the effect of an intravitreal injection of vasohibin-1 protein or the genetic knockout (KO) of vasohibin-1 on laser-induced CNV in rodents.

## METHODS

### Animals

The procedures used in all the animal experiments adhered to the guidelines of the ARVO Statement for the Use of Animals in Ophthalmic and Vision Research and were approved by the Animal Care Committee of Tohoku University Graduate School of Medicine. Male mice between 8 to 12 weeks of age were used. Homozygous vasohibin-1 gene KO mice on a C57BL/6J background were generated by gene targeting, as described.<sup>29</sup> Wild-type (WT) C57BL/6J mice served as controls. For all procedures, the animals were anesthetized with an intraperitoneal injection of 30 mg/kg pentobarbital, and the pupils were dilated with topical 2.5% phenylephrine and 1% tropicamide.

One hundred sixty-two mice were used. Four untreated mice and 12 mice at 4, 14, and 28 days (four per group) after the laser application were used for immunohistochemistry. Thirty mice (five groups, six mice in each group) were used for reverse transcription-polymerase chain reaction (RT-PCR) to determine the natural course of the laser-induced CNV. Twenty-four mice (four groups: untreated, 4, 7, and 14 days after laser application; six mice in each group) for RT-PCR after vasohibin-1 or vehicle injection (24 mice) into the vitreous for laser-induced CNV (eight mice; WT and KO for RT-PCR of vasohibin-1; 4 mice each group); 24 mice (four groups: vasohibin-1 and vehicle injection for WT and KO mice, respectively; six mice in each group) for fluorescein angiography; and 36 mice (six groups with 0, 1, 10, and 100 ng vasohibin-1 injection for WT and vehicle and vasohibin-1 for KO; six mice in each group) for choroidal flat mounts.

### Expression and Purification of Human Vasohibin-1 Protein

Human vasohibin-1 gene with optimized codons for *Escherichia coli* expression was cloned into pET-32 LIC/Xa (Novagen, Madison, WI). The resultant expression plasmid encoded vasohibin-1 with a sequence of GSNPLAMAISDPNSSVDKLAALAEHHHHHHH at its C terminus, as a thio-redoxin fusion protein. *E. coli* BL21(DE3) transformants were cultivated at 37°C in TB medium (2.4% yeast extract, 1.2% tryptone, 1.25% K<sub>2</sub>HPO<sub>4</sub>, 0.23% KH<sub>2</sub>PO<sub>4</sub>, 500 mg/mL polypropylene glycol 2000, and 50 µg/mL ampicillin [pH 7.0]) supplemented with 4% glycerol, and the expression was induced by addition of 1 mM isopropyl-β-D-thiogalactopyranoside (OD<sub>650</sub> = 5). After 16 hours of cultivation, the cells were harvested and disrupted in 20 mM sodium phosphate buffer (pH 7.6), containing 0.5 M NaCl and 1 mM phenylmethylsulfonyl fluoride (PMSF) in a high-pressure homogenizer. The inclusion bodies were collected, washed with the same buffer, and solubilized in 20 mM sodium phosphate buffer (pH 8.0), containing 0.5 M NaCl, 1 mM PMSF, 5 mM 2-mercaptoethanol, 60 mM imidazole, and 7 M guanidine HCl. The soluble fraction was loaded onto a Ni chelating Sepharose column (GE Health care, Princeton, NJ) which was equilibrated with the solubilization buffer. Vasohibin-1 fusion protein was eluted with 20 mM sodium phosphate buffer (pH 8.0), containing 0.5 M NaCl, 1 mM PMSF, 5 mM 2-mercaptoethanol, 300 mM imidazole, and 8 M urea. The eluted protein fraction was then dialyzed against 20 mM glycine-HCl buffer (pH 3.5) and digested with blood coagulation factor Xa (Novagen) for 1 hour at 25°C after the addition of the reaction buffer. The released vasohibin-1 was collected as the insoluble fraction, solubilized, and purified with Ni chelating Sepharose by a method used for fusion proteins. Vasohibin-1 was then collected as an insoluble fraction after

dialysis against 20 mM Tris-HCl buffer (pH 8.0), resolubilized in 25 mM sodium phosphate (pH 7.2) containing 4 M urea, loaded onto a Q Sepharose column (GE Health care), and eluted by linearly increasing the NaCl concentration to 1 M. After vasohibin-1 was dialyzed against 20 mM glycine-HCl buffer (pH 3.5), the protein fraction was recovered as an insoluble fraction by addition of 1 M Tris-HCl buffer (pH 8.0) to 20% volume of the above solution. Vasohibin-1 was resolubilized with 50 mM Tris-HCl buffer containing 50 mM NaCl, 5 mM Tris(2-carboxyethyl)phosphine, 0.5 mM EDTA, 5% glycerol, and 4.4% N-lauroylsarcosine (pH 8.0) and was dialyzed twice against 20 mM sodium phosphate buffer (pH 8.0) and once with PBS, each for at least a day.

The protein concentration was determined by the Bradford method with a protein assay kit (Bio-Rad Laboratories, Hercules, CA), with bovine serum albumin as the standard protein.

### Experimental CNV

An Argon green laser, with a slit lamp delivery system (Ultima 2000SE; Lumenis, Yokneam, Israel) and a coverslip as a contact lens, was used to rupture the choroidal membrane.<sup>30-32</sup> The laser settings were 50-µm diameter, 0.05-second duration, and 150-mW intensity. For fluorescein angiography and choroidal flat-mount examinations, three burns were made in the peripapillary region in a standardized fashion, and each burn was approximately one to two disc diameters from the optic disc.

For RT-PCR and immunohistochemistry, three burns were made around the optic disc with the burns separated by one to two disc diameters. Only eyes in which subretinal bubbles were formed indicating a rupture of the Bruch membrane were studied.

### Immunohistochemistry

WT mice with laser-induced CNV lesions were studied on days 4, 14, and 28 after laser burn for immunostaining of vasohibin-1 (*n* = 4 eyes/group). All procedures were performed at room temperature unless otherwise stated. The eyes were enucleated and fixed for 12 hours in 4% paraformaldehyde (PFA) at 4°C and cryoprotected by successive incubations in 10%, 20%, and 30% sucrose dissolved in saline, for 12 hours each at 4°C. The tissues were immersed in OCT compound (Tissue-Tek; Sakura Finetek, Torrance, CA) and frozen in acetone in a dry ice bath. The frozen eyes were sectioned at 10 µm with a cryostat. Adjacent sections were stained with hematoxylin and eosin (HE).

For double staining with vasohibin-1, antibodies against CD-31 (marker for ECs), CD68 (marker for macrophage), α-smooth muscle actin (αSMA, marker for dedifferentiated RPE), and cytokeratin (marker for RPE) were used. Mouse eyes were enucleated, immersed in OCT compound and frozen in acetone in a dry ice bath. The frozen eyes were sectioned at 10 µm with a cryostat, dried, and fixed in methanol for 10 minutes. After blocking, mouse monoclonal antibodies against mouse vasohibin-1 (1:400)<sup>29</sup> and rat monoclonal antibodies against mouse CD-31 (a marker for ECs; 1:100; BD Biosciences, San Jose, CA), mouse monoclonal anti-CD68 antibody (a marker for macrophages; 1:400; Dako, Hamburg, Germany), mouse monoclonal anti-α-smooth muscle antibody (αSMA, marker for dedifferentiated RPE; 1:400; Thermo Fisher Scientific Inc., Waltham, MA), mouse monoclonal anti-mouse pan-cytokeratin (a marker for RPE; 1:200; pan-cytokeratins/cytokeratin 18 clone CY90; CK18, 1:10; Sigma-Aldrich, St. Louis, MO) were applied to the sections overnight at 4°C. For control experiments, preimmune mouse IgG was used instead of the primary antibody. The sections were incubated in Alexa Fluor 594-conjugated anti-mouse IgG (1:400; Invitrogen, Eugene, OR) and Alexa Fluor 488-conjugated anti-rat IgG (1:100; Invitrogen) for 30 minutes. The sections were washed three times with PBS between each step. The slides were counterstained with 4',6-diamino-1-phenylindole (DAPI; Vector Laboratories, Burlingame, CA) and were photographed with a fluorescence microscope (model FW4000, ver. 1.2.1; Leica Microsystems Japan, Tokyo, Japan).

### Preparation of Total RNA and Real-Time Reverse Transcription-Polymerase Chain Reaction

For semiquantitative RT-PCR, the eyes of male WT mice were enucleated on days 4, 7, 14, and 28 after the laser burns (*n* = 6 eyes/group).

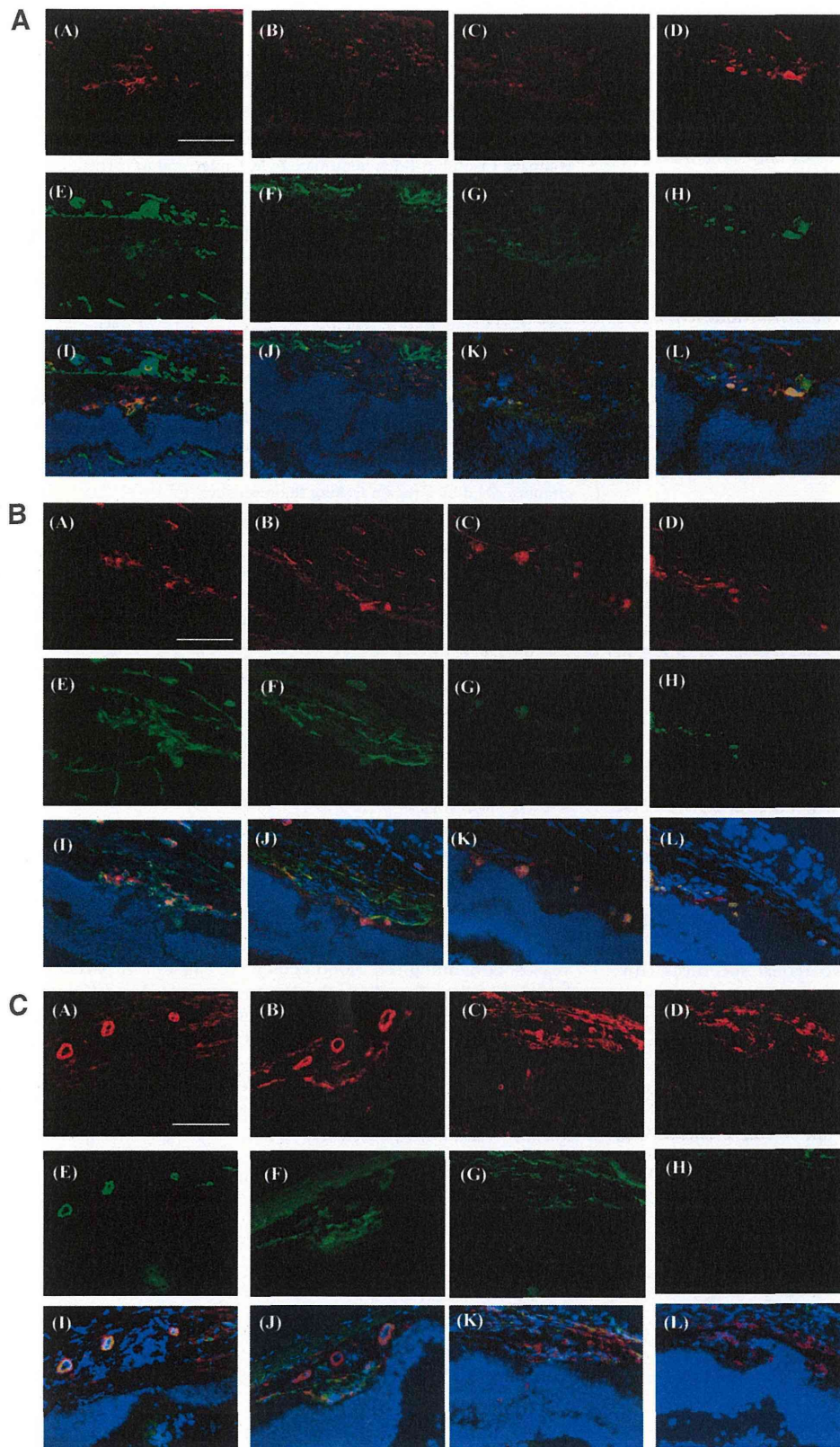


**FIGURE 1.** H&E staining and immunohistochemistry of laser-induced experimental CNV membranes. (A) H&E staining of a mouse eye at 4 days after laser application. A fusiform-shaped CNV is present. Immunohistochemistry for vasohibin-1 in mouse CNV lesions at 4 (1.1), 14 (1.2), and 28 (1.3) days after laser application is shown. (A–D) Vasohibin-1, (E) anti-CD68, (F) anti-cytokeratin, (G) anti- $\alpha$  smooth muscle actin ( $\alpha$ SMA), and (H) anti-CD31, respectively. (I–L) Merged images. Vasohibin-1 was observed on these days, although it seems more intensive on day 28. On day 4, vasohibin was co-expressed with CD68-positive macrophages (1.1A, 1.1E, 1.1I) and CD31-positive endothelial cells (1.1D, 1.1H, 1.1L). These findings are also observed on day 14 after laser application (1.2A, 1.2E, 1.2I, 1.2D, 1.2H, 1.2L). Further vasohibin-1 is co-expressed on  $\alpha$ SMA-positive dedifferentiated RPE (1.2C, 1.2G, 1.2K) and partially with cytokeratin-positive RPE (1.2B, 1.2F, 1.2J). On day 28, vasohibin-1-positive cells were observed on CD31-positive choroidal endothelial cells (1.3D, 1.3H, 1.3L). CD68-positive macrophages were rarely seen on day 28 (1.3A, 1.3E, 1.3I). Cytokeratin-positive RPE was absent at the laser burned area on day 4 (1.1F), but gradually increased on day 14 (1.2F) and covered the CNV on day 28 (1.3F). None of these signals was observed with the control IgG. Bar, 20  $\mu$ m.

Untreated eyes of WT and vasohibin-1 KO mice were also examined for the expression of vasohibin-1 ( $n = 4$  eyes/group). The anterior segment, muscles, optic nerve, and entire retina were removed to isolate the eye cup which included the RPE-choroid-sclera complex. Each

tissue was separately mixed with denaturing solution, and mRNA was prepared (QuickPrep micromRNA Purification Kit; Amersham Biosciences, Buckinghamshire, UK), according to the manufacturer's instructions. The purified mRNA was reverse-transcribed to cDNA using

(First-Strand cDNA Synthesis Kit; Amersham Biosciences). One microliter of cDNA was used for real-time PCR amplification on a thermocycler (Light Cycler; Roche, Meylan, France, and the Light Cycler FastStart DNA Master SYBR Green I Reagent Kit; Roche).

The sequences of the PCR primer pairs were: VEGF, 5'-TCT GCT CTC TTG GGT GCA AT-3' (forward) and 5'-TTC CGG TGA GAG GTC CGG TT-3' (reverse); vasohibin-1, 5'-GAT TCC CAT ACC AAG TGT GCC-3' (forward), and 5'-ATG TGG CGG AAG TAG TTC CC-3' (reverse); VEGFR1, 5'-GAGGAGGATGAGGGTGTCTATAGGT-3' ACC AAG TGT GCC 5'-GTGATCAGCTCCAGGTTTGACTT-3' ACC AAG TGT-VEGFR2, 5'-GCCCTGCCTGTGGTCTCACTAC-3' ACC AAG TGT G5'-CAAAGCATTGCCATTCGAT-3' (reverse); PEDF, 5'-AGCTGAACATCGAACAGAGT-3' (forward) and 5'-CGAAGTTTCTCTCAAACAC-3' (reverse); glyceraldehyde-3-phosphate-dehydrogenase (GAPDH), 5'-AAG GTG AAG GTC GGA GTC AA-3' (forward), 5'-TTG AGG TCA ATG AAG GGG TC-3'.

The PCR conditions were: 95°C for 10 minutes; 95°C for 10 seconds; hybridization temperature for 10 seconds (VEGF, 66°C; vasohibin-1, 62°C; VEGFR1-1, 57°C; VEGFR2, 56°C; PEDF, 50°C; and GAPDH, 55°C); and 72°C for 10 seconds. The second step was repeated for 45 cycles. All data were normalized to GAPDH expression, thus giving the relative expression level.

### Intravitreal Injection of Recombinant Vasohibin Protein

Male WT mice were injected intravitreally in both eyes with 1, 10, or 100 ng/1  $\mu$ L recombinant vasohibin-1 protein<sup>24-26,29</sup> 4 days after the laser burn. One microliter of PBS was used as vehicle. The mice were anesthetized, the pupils were dilated, and the intravitreal injections were made with a 32-gauge needle attached to a 5- $\mu$ L glass syringe (Hamilton, Reno, NV). The needle was passed through the sclera just behind the limbus into the vitreous cavity.

### Fluorescein Angiography

Fluorescein angiography (FA) was used to determine the activity of the CNV lesion and to investigate the efficacy of vasohibin-1 protein injection in both WT and vasohibin-1 KO mice ( $n = 8$  eyes/group).<sup>30</sup> FA was performed with a camera and imaging system (Genesis-Df; Kowa, Tokyo, Japan) 2 weeks after the laser photocoagulation. Photographs were taken with a 20-D lens in contact with the fundus camera lens after an intraperitoneal injection of 0.1 mL of 2% fluorescein sodium (Sigma-Aldrich). Two retinal specialists (RW, TA) evaluated the angiograms in a masked fashion. Lesions were graded according to an established scheme: 0, no leakage with faint hyperfluorescence or mottled fluorescence without leakage; 1, questionable leakage with hyperfluorescent lesion but no increase in size or intensity; 2A, leaky with hyperfluorescence increasing in intensity but not in size; and 2B, pathologically significant leakage with hyperfluorescence increasing in intensity and in size.<sup>31</sup> The CNV ac-

tivity in the FA images was calculated for each of the three burns in each eye and summed.

### Fluorescein-Labeled Dextran Perfusion and Choroidal Flat-Mount Preparation

The size of the CNV lesion was measured in choroidal flat mounts to compare vasohibin-1-deficient mice to WT mice and to investigate the efficacy of vasohibin-1 protein injection ( $n = 10$  eyes/group). On day 14, after the laser application, the mice were perfused with 0.5 mL PBS containing 50 mg/mL fluorescein-labeled dextran (FITC-dextran; MW  $2 \times 10^6$ ; Sigma Aldrich). The eyes were removed and fixed for 30 minutes in 4% phosphate-buffered PFA. The cornea and lens were removed, and the entire retina was carefully dissected from the eye cup. Radial cuts (four to six) were made from the edge to the equator, and the eye cup of the RPE-choroid-sclera complex was flat mounted (Permalfluor; Beckman Coulter, Fullerton, CA) with the sclera side facing down. Flat mounts were examined by fluorescence microscopy (model FW4000, ver. 1.2.1; Leica Microsystems Japan), and the total area of each CNV associated with each burn was measured. The CNV lesions were identified by the fluorescent blood vessels on the choroid-retinal interface circumscribed by a region lacking fluorescence.<sup>31,32</sup>

### Statistical Analyses

Analysis of variance (ANOVA) with the Scheffé test for post hoc analysis was used to examine the differences in the relative expression levels of each gene. Differences in the incidence of grade 2B lesions between WT and KO mice, and between different dosages of intravitreal vasohibin-1 injections were analyzed by  $\chi^2$  tests. The size of CNV was compared between groups using the Student's two-sample *t*-tests.

## RESULTS

### Histology and Immunostaining of CNV

We followed the natural course of laser-induced CNVs in the WT mice. The HE-stained sections of WT mice showed the same pattern in the development of CNV as described in another study.<sup>32</sup> On day 4 after the laser application, a fusiform-shaped lesion developed that consisted primarily of pigment-laden cells, fibroblasts, ECs, and RPE cells. Small new vessels containing red blood cells were present in parts of the lesion. On days 7 and 14, the lesion was larger and the blood vessels had increased in size and number (data not shown).

Vasohibin-1 was detected in CD31-positive cells on all days examined (Figs. 1.1, 1.2, 1.3: A, E, D). However, the expression seemed to be stronger on day 28 after the laser burn. Vasohibin-1 was also detected in CD68-positive cells on days 4 (Figs. 1.1A, 1.1E, 1.1I) and 14 (Figs. 1.2A, 1.2E, 1.2I). CD68-positive

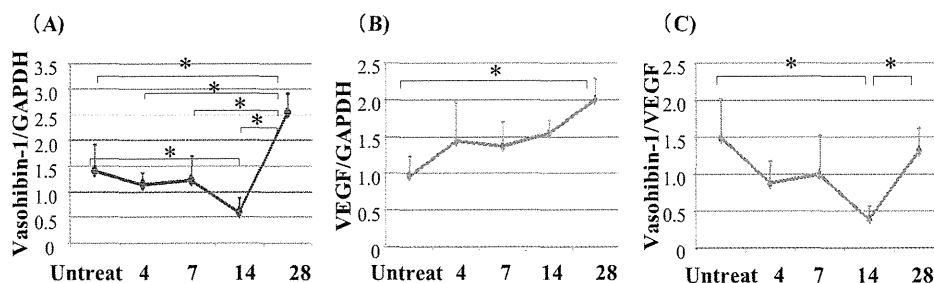


**FIGURE 2.** Semiquantitative RT-PCR of wild-type mouse eyes after laser application. The level of expression of vasohibin-1 (A) and vascular endothelial growth factor (VEGF) (B) is normalized to that of glyceraldehyde-3-phosphate-dehydrogenase (GAPDH). Vasohibin-1 expression decreases until 14 days after laser application, and then markedly increases on day 28. VEGF expression increases gradually until 28 days after laser application. The ratio of vasohibin-1/VEGF expression decreased until 14 days after laser and then increased at day 28 (C). \* $P < 0.05$ .

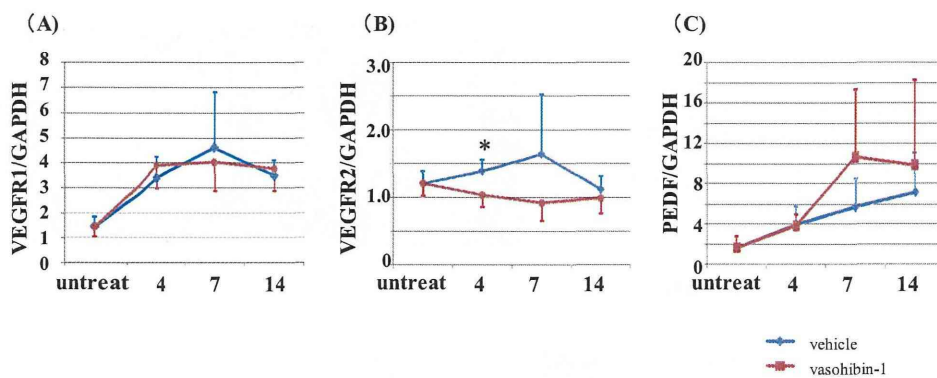


**FIGURE 3.** Semiquantitative RT-PCR for VEGFR1, VEGFR2, and PEDF are shown. VEGFR1 expression is not significantly different between vasohibin-1- and vehicle-treated eyes (A). Significantly lower levels of VEGFR2 expression were observed on day 4 after laser application between vasohibin-1- and vehicle-treated eyes (B, asterisk). PEDF expression was not significantly different between vasohibin-1- and vehicle-treated eyes (C).

cells were rarely observed on day 28. Vasohibin-1 was also detected in  $\alpha$ SMA-positive cells on day 14 (Figs. 1.2C, 1.2G, 1.2K). A weak expression of vasohibin-1 was also detected in cytokeratin-positive cells on days 14 and 28 (Figs. 1.2, 1.3: B, F, J). Our preliminary study showed that RPE cell lines, such as RPE-J and ARPE, expressed the vasohibin-1 gene (data not shown). Our results therefore showed that ECs and macrophages, dedifferentiated RPE, and perhaps some of the differentiated RPE may express vasohibin-1.

#### Real-Time RT-PCR

The results of real-time RT-PCR in WT mice are shown in Figure 2. The level of vasohibin-1 expression decreased until day 14 after the laser application and then was markedly increased on day 28 (Fig. 2A). Thus, the mean ratio of the mRNA expression of vasohibin-1/GAPDH was  $1.403 \pm 0.503$  before the laser application,  $1.14 \pm 0.239$  on day 4 after laser application,  $1.226 \pm 0.080$  on day 7,  $0.593 \pm 0.119$  on day 14, and  $2.552 \pm 0.147$  on day 28. Statistical analyses showed that vasohibin-1 expression on day 28 was significantly higher than in untreated eyes ( $P = 0.001$ ) or on days 4 ( $P < 0.0001$ ), 7 ( $P = 0.0001$ ), and 14 ( $P < 0.0001$ ). The lower expression observed on day 14 than that of untreated eyes was significant ( $P = 0.0277$ ).

Conversely, the VEGF expression increased gradually until 28 days after the laser application (Fig. 2B). Thus, the mean ratio of the mRNA level of VEGF was  $0.962 \pm 0.265$  before laser application, and  $1.436 \pm 0.522$  at day 4,  $1.358 \pm 0.335$  at day 7,  $1.539 \pm 0.175$  at day 14, and  $1.996 \pm 0.289$  at day 28. At day 28 after laser application, the VEGF levels were significantly higher than in the untreated eyes ( $P = 0.0006$ ). The ratio of vasohibin/VEGF expression (Fig. 2C) was  $1.484 \pm 0.54$  without laser,  $0.877 \pm 0.298$  at day 4 after laser,  $0.989 \pm 0.537$  at day 7,  $0.384 \pm 0.178$ , at day 14, and  $1.314 \pm 0.316$  on day 28. Thus, the ratio decreased until day 14 after the laser application and then returned to the normal level on day 28. The vasohibin/VEGF level on day 14 was significantly lower than that in the untreated eyes ( $P = 0.0022$ ) and on day 28 ( $P = 0.0116$ ).

The results of real-time PCR for VEGFR1 in WT mice showed that VEGFR1 expression was not significantly different between vasohibin-1 injected and vehicle injected eyes (Fig. 3A). The expression of VEGFR2 in vasohibin-1-treated eyes was significantly lower than that in vehicle-treated eyes 4 days after the laser application (Fig. 3B, asterisk;  $P = 0.013$ ). The expression of PEDF in the vasohibin-1 treated eyes was not significantly different from that in vehicle-treated eyes (Fig. 3C).

#### Angiographic Leakage from CNV

Fluorescein angiography showed that an intravitreal injection of 10 ng recombinant vasohibin-1 protein on day 4 after laser application led to a significant reduction in the size of the CNV.

On day 14, significant pathologic leakage (grade 2B lesions) was observed in 57.1% of the lesions in control mice, but in only 8.3% of the lesions in the treated mice ( $P = 0.0002$ ; Fig. 4).

We performed the same experiments in vasohibin-1 KO mice. The fundus, histologic, and ERG examinations showed that the morphologic architecture and function of vasohibin-1 KO mice did not differ from those of wild-type mice under normal conditions (data not shown). Vasohibin was expressed in retinal and choroidal vessels by immunostaining and RT-PCR analyses. Conversely, vasohibin-1 was not detected in the mutant eyes (Fig. 5A). Comparisons of the fluorescein angiograms showed that vasohibin-1 KO mice developed larger and leakier

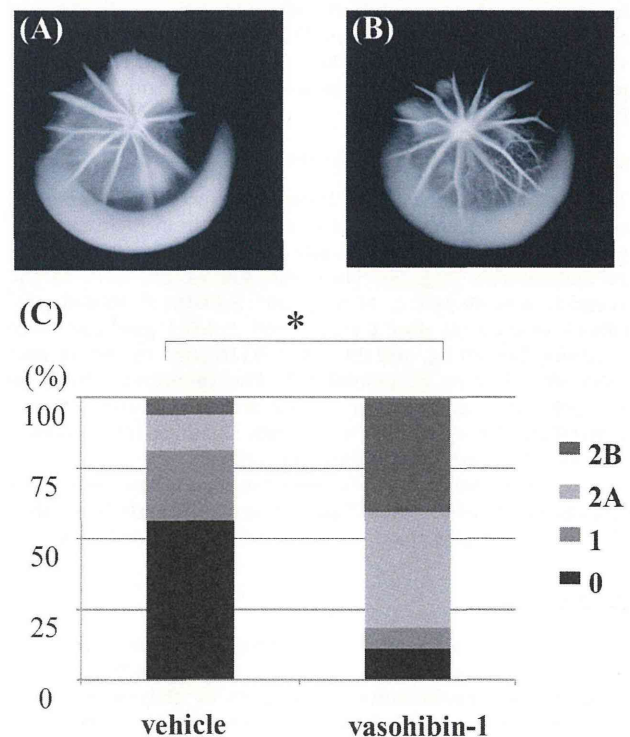


**FIGURE 4.** Angiographic leakage from CNV lesions with and without intravitreal injection of 10 ng recombinant vasohibin-1 protein 4 days after laser application. (A) Representative fluorescein angiogram of vehicle-injected eyes. Active CNV can be seen as a large hyperfluorescent area. (B) Representative fluorescein angiogram of vasohibin-1-injected eyes. Small and less leaky CNVs indicate the inhibitory effect of vasohibin-1. (C) Histogram of angiographic leakage grades. A significantly lower numbers of grade 2B lesions occur in vasohibin-1-injected eyes than in control eyes 2 weeks after laser induction ( $P < 0.001$ ,  $\chi^2$  test).

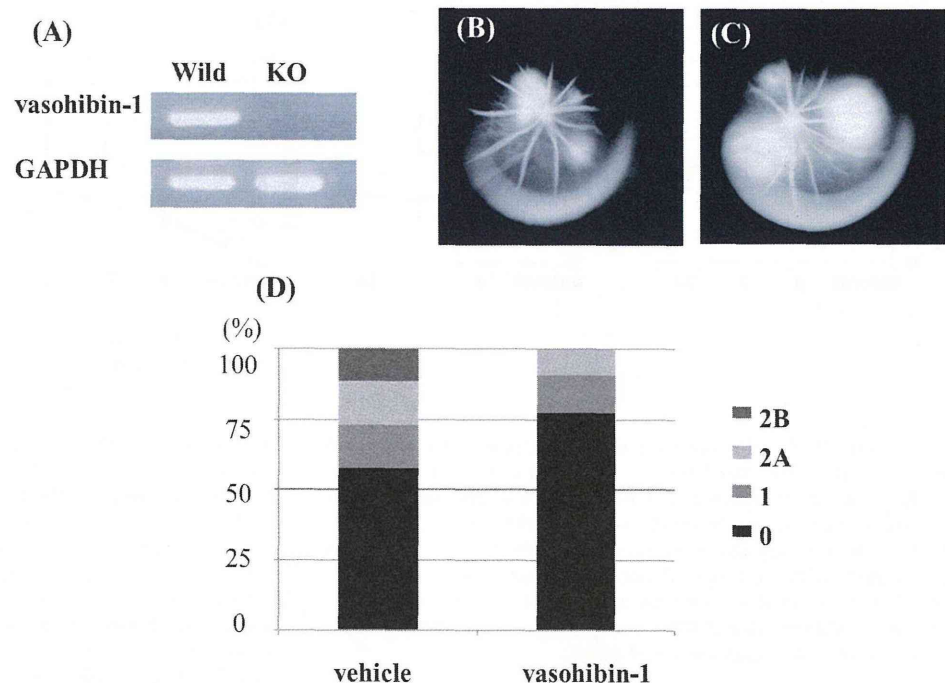


**FIGURE 5.** (A) RT-PCR analysis of vasohibin-1 and glyceraldehyde-3-phosphate-dehydrogenase (GAPDH) mRNA in the eyes of wild-type or KO mice. Vasohibin-1 was not detected in the KO eye. Angiographic leakage from CNV lesions in the eyes of wild-type or vasohibin-1 KO mice. (B, C) Representative fluorescein angiogram of wild-type eyes and vasohibin-1-KO eyes, respectively, showing larger and leakier CNV lesions in KO compared with wild-type. (D) Histogram of angiographic leakage grades. More grade 2B lesions occurred in vasohibin-1-KO eyes than in wild-type eyes 2 weeks after laser induction, but the difference is not statistically significant ( $P = 0.097$ ,  $\chi^2$  test).

CNVs than did the WT mice (Figs. 5B, 5C). On day 14, grade 2B lesions were observed in 55.0% of the lesions in WT mice and a higher percentage (81.2%) of 2B lesions were detected in the vasohibin-1 deficient mice. However, the difference in the percentages of grade 2B lesions was not significant ( $P = 0.097$ , Fig. 5D).

### Size of CNVs in Flat Mounts

The size of the induced CNV lesions measured in flat-mounted choroids was smaller in eyes that received an intravitreal injection of vasohibin-1 protein on day 4 after laser application than in the controls (Fig. 6). Thus, the size of the CNV in the controls was  $49,926 \pm 11,837 \mu\text{m}^2$ ;  $34,019 \pm 10,048 \mu\text{m}^2$  (68.1% of control) after 1 ng,  $20,465 \pm 6541 \mu\text{m}^2$  (40.9% of control) after 10 ng, and  $23,733 \pm 5116 \mu\text{m}^2$  (47.5% of control) after 100 ng of vasohibin-1. The differences between control and 1 ng, between control and 10 ng, and between control and 100 ng were all statistically significant ( $P = 0.0002$ ,  $<0.0000001$ , and  $<0.0000001$ , respectively).

The mean size of the CNV lesions in the eyes of vasohibin-1 KO mice ( $105,140 \pm 34,447 \mu\text{m}^2$ ) was significantly larger than that in the WT ( $49,176 \pm 15,455 \mu\text{m}^2$ ;  $P = 0.00001$ ; Fig. 7).

### DISCUSSION

Vasohibin-1 is expressed in a wide range of tissues and organs in embryos and adults.<sup>24,33</sup> It is also expressed on human CNV membranes,<sup>28</sup> proliferative membranes of diabetic retinopathy,<sup>34</sup> and blood vessels in tumors.<sup>35</sup> Our results showed that vasohibin-1 was expressed, not only on the endothelial cells but also on macrophages, dedifferentiated RPE cells, and probably on RPE cells. The expression seemed to increase after the laser application. When we examined the vasohibin-1 expression on day 28 after laser application, strong vasohibin-1 expression was observed only on the CNV lesion, although weak expression was always observed on the RPE cells.  $\alpha$ SMA-positive dedifferentiated RPE cells also expressed vasohibin-1 on day 14, and histologic examination showed that regressed CNV lesions were covered with cytokeratin-positive RPE cells on

day 28. These results show that vasohibin-1 expression may play a role in the regression of CNV, as we reported.<sup>28</sup>

When the CNV was created around the optic disc (three spots in each eye), each spot did not have the same degree of FA leakage. From our experimental design, it was very difficult to detect significant differences in the vasohibin-1/VEGF ratio for each spot. Alternatively, we determined the vasohibin-1/VEGF ratio during the following days. RT-PCR showed that the vasohibin-1 expression was significantly decreased on 14 days after laser application and then increased above normal level on day 28. This result agrees with the reports that laser-induced CNV lesion enlarges and matures between days 7 to 14 after laser application.<sup>31,36</sup> The results of RT-PCR for vasohibin-1/VEGF ratio show comparable results. From these results, we suggest that the growth and the maturation of the CNV lesions may partially correlate with the vasohibin-1 and VEGF expression levels.

Although vasohibin-1 expression is stimulated by VEGF, VEGF receptor 2, and the protein kinase C delta (PKC $\delta$ ) pathway,<sup>27</sup> other proangiogenic and antiangiogenic factors may modify the expression of vasohibin-1 during the course of the CNV development. It has been reported that not only VEGF, but also bFGF, placenta growth factor, and hepatocyte growth factor increase the expression of vasohibin-1.<sup>24,27</sup> TNF- $\alpha$ , interleukin (IL)-1, and hypoxia inhibit the VEGF-stimulated vasohibin-1 expression in vitro.<sup>24,27</sup> The macrophage-like mononuclear cells in human CNVs have been reported to produce TNF- $\alpha$  and IL-1 $\beta$ .<sup>8</sup> Shi et al.<sup>37</sup> reported the expression of TNF- $\alpha$  was 4.57-fold higher in the choroid and RPE of eyes with a laser-induced CNV than in the eyes of controls. In addition, pretreatment of these eyes with anti-TNF- $\alpha$  agents significantly reduced the size of the CNV and the pathologic fluorescein leakage. We also observed macrophages in the CNVs until day 14 which showed that the CNV lesions were still active but rarely on day 28 when the CNV had already regressed.

It has been reported that choroidal blood flow and the permeability of Bruch's membrane is decreased in the eyes of the elderly, especially patients with AMD, resulting in a hypoxic environment surrounding the choroidal ECs.<sup>38-40</sup> Hyp-

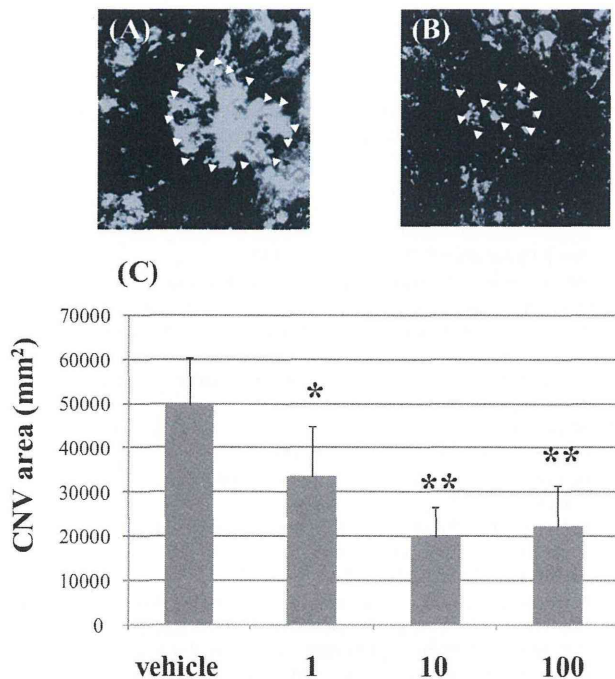


**FIGURE 6.** Size of CNV membranes, with or without intravitreal injection of recombinant vasohibin-1 protein, 4 days after laser application. (A) Representative choroidal flat-mount photograph of vehicle-injected eyes. (B) Representative choroidal flat-mount photograph of eyes injected with 10 ng of vasohibin-1 protein. *Small arrowheads*: CNV lesion. (C) Choroidal flat-mount examination 2 weeks after laser induction after 1, 10, and 100 ng of vasohibin-1 protein suppresses the growth of the CNVs. Vasohibin-1 suppressed CNV at 32% by 1 ng, 59% by 10 ng, and 52% by 100 ng, when compared to that of vehicle injection. \* $P < 0.001$ , \*\* $P < 0.0000001$ , Student's two-sample *t*-tests compared with vehicle-injected eyes.

oxia increases the expression of VEGF and matrix metalloproteinase in choroidal ECs, and this may facilitate the formation and recurrences of CNVs.<sup>41</sup> Hypoxia may also change the vasohibin-1 expression. We suggest that the regulation of vasohibin-1 expression may change the natural course of CNV in patients with AMD.<sup>28</sup>

Our results showed that an intravitreal injection of vasohibin-1 significantly reduced the size of the CNVs, and vasohibin-1 KO mice had larger CNVs than that of WT mice. Ida et al.<sup>42</sup> reported that despite a continuous high expression of VEGF and its receptors, subretinal neovascularizations stopped growing and reached a plateau in rho/VEGF transgenic mice. These results show that not only the withdrawal of angiogenic stimulation by VEGF, but also antiangiogenic factors, including vasohibin-1, play a role in CNV regression during its natural course.

Many other endogenous antiangiogenic factors, such as PEDF, a 50-kDa noninhibitory member of the serine protease inhibitor gene family, must be considered.<sup>43,44</sup> PEDF is expressed in RPE cells, CNV membranes, corneal cells, and ciliary epithelial cells.<sup>9,44</sup> The concentration of PEDF in the vitreous and aqueous decreases with increasing age and is very low in AMD patients.<sup>45</sup> It has been reported that the level of PEDF in CNV membranes increases after stimulation of the VEGF receptor 1.<sup>46</sup> This effect may be a negative feedback loop against the VEGF-induced neovascularization. Studies using gene transfer have demonstrated that PEDF suppresses the development of CNVs.<sup>47,48</sup> Our real-time PCR results confirmed these findings that the expression of PEDF also increased during the CNV enlargement until day 14. The level of PEDF expression was

opposite that of vasohibin-1 expression. However, vasohibin-1 injection did not induce significant differences in the PEDF expression from that obtained with vehicle injection. Vasohibin-1 was suspected to suppress CNV, in addition to PEDF signaling. Apte et al.<sup>49</sup> reported that low doses of PEDF are inhibitory in experimental CNV, whereas high doses enhance the development of neovascularization. A maximum dose of intravitreal 100 ng vasohibin-1, which is 10 times the amount with the maximum effect, did not reverse the effect of PEDF under our experimental conditions. Vasohibin-1 may be safer than PEDF for antiangiogenesis in our experimental condition.

Although a complete understanding of the angiogenic inhibition by vasohibin-1 has not been attained, Shen et al.<sup>26</sup> reported that vasohibin-1 suppressed retinal neovascularization and suggested that a downregulation of the VEGF receptor 2 gene may play some role in mediating its activity. Zhou et al.<sup>50</sup> reported a significant reduction of corneal neovascularization by alkali-treated mice cornea. They showed a significant decrease of in VEGFR2 gene expression during the experimental period and suggested that there is an important correlation in the downregulation of VEGFR2 and vasohibin-1. When we examined the gene expression of VEGFR1 and -R2, significantly less VEGFR2 expression was observed in the vasohibin-1-treated eyes at day 4 after laser application, although the results may have been affected by the number of animals ( $n = 6$ ). Although we could not examine the VEGF-mediated tyrosine phosphorylation of VEGFR2 from our small samples, we suggest that external vasohibin-1 plays some role in the antiangiogenesis by a downregulation of VEGFR2, together with the earlier findings. These observations also imply a synergistic effect of anti-VEGF agents and vasohibin-1 against CNV growth.

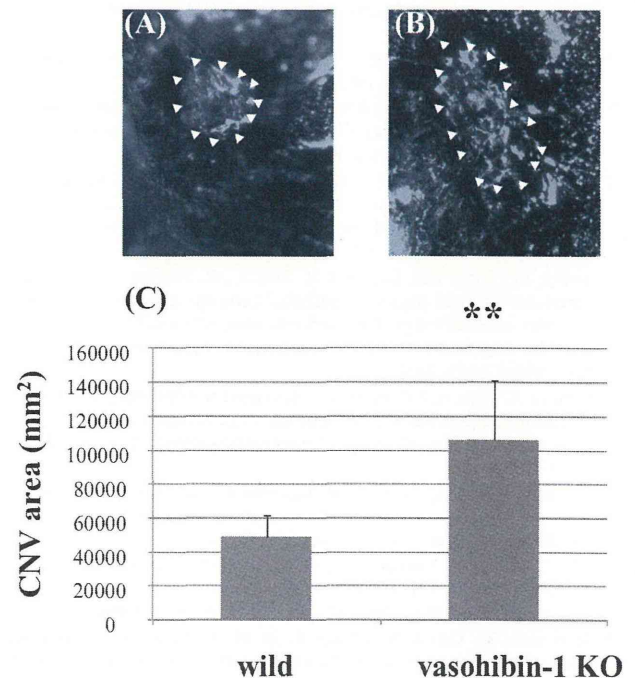


**FIGURE 7.** Size of CNV lesions in the eyes of wild-type or vasohibin-1-KO mice. (A) Representative choroidal flat-mount photograph of wild-type eye. (B) Representative choroidal flat-mount photograph of vasohibin-1-KO eye. *Arrowheads*: the CNV. (C) Choroidal flat-mount examination 2 weeks after laser induction shows CNVs in the eyes of vasohibin-1-KO mice are two times (213.8%) larger than that of wild-type eyes. \*\* $P < 0.0001$ , Student's two-sample *t*-test, compared with wild-type eyes.

When we injected vasohibin-1 intravitreally on days 1, 4, and 7 after laser application, we found that eyes that received vasohibin-1 on day 4 had better results than those at the other days. This is the reason that we injected vasohibin-1 4 days after the laser application. Vasohibin is thought to work in an autocrine manner<sup>24,25</sup> with a small vasohibin-binding protein.<sup>51</sup> The half-life of vasohibin-1 is short, approximately 5 minutes (Sato Y, personal communication, 2010), after systemic application. However, the half-life of vasohibin-1 in the eye is unknown. It may be very short and may correlate with the timing of vasohibin-1 application at 4 days after laser application, under our experimental conditions. Alternatively, our experimental condition may have affected the results. In any case, when we consider the optimum day for the vasohibin injection, it may be different from that of anti-VEGF agents. This reason may be another explanation for the synergistic effect of anti-VEGF agents and vasohibin-1 against CNV growth.

In conclusion, the endogenous expression of vasohibin-1 is associated with the natural course of the development of a CNV. Vasohibin-1 was expressed on ECs, macrophages, and weakly on RPE cells, and especially on active CNV lesions. External vasohibin-1 application may alter the development of experimental mice CNVs, and we recommend that vasohibin-1 be considered to as a treatment to suppress CNV growth.

### Acknowledgments

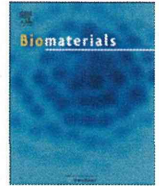
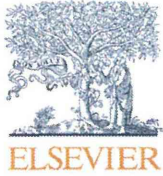
The authors thank Kota Sato and Haruka Seto for excellent technical assistance.

### References

- Klein R, Peto T, Bird AC, Vannewkirk MR. The epidemiology of age-related macular degeneration. *Am J Ophthalmol*. 2004;137:486–495.
- Bressler NM, Bressler SB, Fine SL. Age-related macular degeneration. *Surv Ophthalmol*. 1998;32:375–413.
- Amin R, Puklin JE, Frank RN. Growth factor localization in choroidal neovascular membranes of age-related macular degeneration. *Invest Ophthalmol Vis Sci*. 1994;35:3178–3188.
- Frank RN, Amin RH, Elliott D, Puklin JE, Abrams GW. Basic fibroblast growth factor and vascular endothelial growth factor are present in epiretinal and choroidal neovascular membranes. *Am J Ophthalmol*. 1996;122:393–403.
- Lopez PF, Sippy BD, Lambert M, Thach AB, Hinton DR. Transdifferentiated retinal pigment epithelial cells are immunoreactive for vascular endothelial growth factor in surgically excised age-related macular degeneration-related membranes. *Invest Ophthalmol Vis Sci*. 1996;37:855–868.
- Kvanta A, Algvere PV, Berglin L, Seregard S. Subfoveal fibrovascular membranes in age-related macular degeneration express vascular endothelial growth factor. *Invest Ophthalmol Vis Sci*. 1996;37:1929–1934.
- Otani A, Takagi H, Oh H, et al. Vascular endothelial growth factor family and receptor expression in human choroidal neovascular membranes. *Microwasc Res*. 2002;64:162–169.
- Oh H, Takagi H, Takagi C, et al. The potential angiogenic role of macrophages in the formation of choroidal neovascular membranes. *Invest Ophthalmol Vis Sci*. 1999;40:1891–1898.
- Matsuoka M, Ogata N, Otsuji T, et al. Expression of pigment epithelium derived factor and vascular endothelial growth factor in choroidal neovascular membranes and polypoidal choroidal vasculopathy. *Br J Ophthalmol*. 2004;88:809–815.
- Grisanti S, Tatar O. The role of vascular endothelial growth factor and other endogenous interplayers in age-related macular degeneration. *Prog Retin Eye Res*. 2008;27:372–390.
- Spilisbury K, Garrett KL, Shen WY, Constable IJ, Rakoczy PE. Overexpression of vascular endothelial growth factor (VEGF) in the retinal pigment epithelium leads to the development of choroidal neovascularization. *Am J Pathol*. 2000;157:135–144.
- Krzystolik MG, Afshari MA, Adamis AP, et al. Prevention of experimental choroidal neovascularization with intravitreal anti-vascular endothelial growth factor antibody fragment. *Arch Ophthalmol*. 2002;120:338–346.
- Rosenfeld PJ, Brown DM, Heier JS, et al. MARINA Study Group. Ranibizumab for neovascular age-related macular degeneration. *N Engl J Med*. 2006;355:1419–1431.
- Regillo CD, Brown M, Abraham P, et al. PIER Study Group. Randomized, double-masked, sham-controlled trial of ranibizumab for neovascular age-related macular degeneration: PIER study year 1. *Am J Ophthalmol*. 2008;145:239–248.
- Pilli S, Kotsolis A, Spaide RF, et al. Endophthalmitis associated with intravitreal anti-vascular endothelial growth factor therapy injections in an office setting. *Am J Ophthalmol*. 2008;145:879–882.
- Lux A, Llacer H, Heussen FMA, Joussen AM. Non-responders to bevacizumab (Avastin) therapy of choroidal neovascular lesions. *Am J Ophthalmol*. 2007;91:1318–1322.
- Alon T, Hemo I, Itin A, Pe'er J, Stone J, Keshet E. Vascular endothelial growth factor acts as a survival factor for newly formed retinal vessels and has implications for retinopathy of prematurity. *Nat Med*. 1995;1:1024–1028.
- Robinson GS, Ju M, Shih SC, et al. Nonvascular role for VEGF: VEGFR1, 2 activity is critical for neural retinal development. *FASEB J*. 2001;15:1215–1217.
- Marneros AG, Fan J, Yokoyama Y, Gerber HP, Ferrara N, Crouch RK, Olsen BR. Vascular endothelial growth factor expression in the retinal pigment epithelium is essential for choriocapillaris development and visual function. *Am J Pathol*. 2005;167:1451–1459.
- Nishijima K, Ng YS, Zhong L, et al. Vascular endothelial growth factor-A is a survival factor for retinal neurons and a critical neuroprotectant during the adaptive response to ischemic injury. *Am J Pathol*. 2007;171:53–67.
- Saint-Geniez M, Maharaj AS, Walshe TE, et al. Endogenous VEGF is required for visual function: evidence for a survival role on Müller cells and photoreceptors. *PLoS One*. 2008;3:e3554.
- Boyer DS, Heier JS, Brown DM, et al. A phase IIIb study to evaluate the safety of ranibizumab in subjects with neovascular age-related macular degeneration. *Ophthalmology*. 2009;116:1731–1739.
- Ueno S, Pease ME, Wersinger DM, et al. Prolonged blockade of VEGF family members does not cause identifiable damage to retinal neurons or vessels. *J Cell Physiol*. 2008;217:13–22.
- Watanabe K, Hasegawa Y, Yamashita H, et al. Vasohibin as an endothelium-derived negative feedback regulator of angiogenesis. *J Clin Invest*. 2004;114:898–907.
- Sonoda H, Ohta H, Watanabe K, et al. Multiple processing forms and their biological activities of a novel angiogenesis inhibitor vasohibin. *Biochem Biophys Res Commun*. 2006;342:640–646.
- Shen J, Yang X, Xiao WH, et al. Vasohibin is up-regulated by VEGF in the retina and suppresses VEGF receptor 2 and retinal neovascularization. *FASEB J*. 2006;20:723–725.
- Shimizu K, Watanabe K, Yamashita H, et al. Gene regulation of a novel angiogenesis inhibitor, vasohibin, in endothelial cells. *Biochem Biophys Res Commun*. 2005;327:700–706.
- Wakusawa R, Abe T, Sato H, et al. Expression of vasohibin, an antiangiogenic factor, in human choroidal neovascular membranes. *Am J Ophthalmol*. 2008;146:235–243.
- Kimura H, Miyashita H, Suzuki Y, et al. Distinctive localization and opposed roles of vasohibin-1 and vasohibin-2 in the regulation of angiogenesis. *Blood*. 2009;113:4810–4818.
- Tobe T, Ortega S, Luna JD, et al. Targeted disruption of the FGF2 gene does not prevent choroidal neovascularization in a murine model. *Am J Pathol*. 1998;153:1641–1646.
- Yu HG, Liu X, Kiss S, et al. Increased choroidal neovascularization following laser induction in mice lacking lysyl oxidase-like 1. *Invest Ophthalmol Vis Sci*. 2008;49:2599–2605.
- Edelman JL, Castro MR. Quantitative image analysis of laser-induced choroidal neovascularization in rat. *Exp Eye Res*. 2000;71:523–533.
- Nimmagadda S, Geetha-Loganathan P, Pröls F, et al. Expression pattern of vasohibin during chick development. *Dev Dyn*. 2007;236:1358–1362.



34. Sato H, Abe T, Wakusawa R, et al. Vitreous levels of vasohibin-1 and vascular endothelial growth factor in patients with proliferative diabetic retinopathy. *Diabetologia*. 2009;52:359-361.
35. Hosaka T, Kimura H, Heishi T, et al. Vasohibin-1 expression in endothelium of tumor blood vessels regulates angiogenesis. *Am J Pathol*. 2009;175:430-439.
36. Odergren A, Ming Y, Kvanta A. Photodynamic therapy of experimental choroidal neovascularization in the mouse. *Curr Eye Res*. 2006;31:765-774.
37. Shi X, Semkova I, Müther PS, et al. Inhibition of TNF-alpha reduces laser-induced choroidal neovascularization. *Exp Eye Res*. 2006;83:1325-1334.
38. Ito YN, Mori K, Young-Duvall J, Yoneya S. Aging changes of the choroidal dye filling pattern in indocyanine green angiography of normal subjects. *Retina*. 2001;21:237-242.
39. Ross RD, Barofsky JM, Cohen G, et al. Presumed macular choroidal watershed vascular filling, choroidal neovascularization, and systemic vascular disease in patients with age-related macular degeneration. *Am J Ophthalmol*. 1998;125:71-80.
40. Chen JC, Fitzke FW, Pauleikhoff D, Bird AC. Functional loss in age-related Bruch's membrane change with choroidal perfusion defect. *Invest Ophthalmol Vis Sci*. 1992;33:334-340.
41. Ottino P, Finley J, Rojo E, et al. Hypoxia activates matrix metalloproteinase expression and the VEGF system in monkey choroid-retinal endothelial cells: Involvement of cytosolic phospholipase A2 activity. 1. *Mol Vis*. 2004;10:341-350.
42. Ida H, Tobe T, Nambu H, et al. RPE cells modulate subretinal neovascularization, but do not cause regression in mice with sustained expression of VEGF. *Invest Ophthalmol Vis Sci*. 2003;44:5430-5437.
43. Dawson DW, Volpert OV, Gillis P, et al. Pigment epithelium-derived factor: a potent inhibitor of angiogenesis. *Science*. 1999;285:245-248.
44. Tong JP, Yao YF. Contribution of VEGF and PEDF to choroidal angiogenesis: a need for balanced expressions. *Clin Biochem*. 2006;39:267-276.
45. Holekamp NM, Bouck N, Volpert O. Pigment epithelium-derived factor is deficient in the vitreous of patients with choroidal neovascularization due to age-related macular degeneration. *Am J Ophthalmol*. 2002;134:220-227.
46. Ohno-Matsui K, Yoshida T, Uetama T, Mochizuki M, Morita I. Vascular endothelial growth factor upregulates pigment epithelium-derived factor expression via VEGFR-1 in human retinal pigment epithelial cells. *Biochem Biophys Res Commun*. 2003;303:962-967.
47. Mori K, Gehlbach P, Ando A, et al. Regression of ocular neovascularization in response to increased expression of pigment epithelium-derived factor. *Invest Ophthalmol Vis Sci*. 2002;43:2428-2434.
48. Campochiaro PA, Nguyen QD, Shah SM, et al. Adenoviral vector-delivered pigment epithelium-derived factor for neovascular age-related macular degeneration: results of a phase I clinical trial. *Hum Gene Ther*. 2006;17:167-176.
49. Apte RS, Barreiro RA, Duh E, Volpert O, Ferguson TA. Stimulation of neovascularization by the anti-angiogenic factor PEDF. *Invest Ophthalmol Vis Sci*. 2004;45:4491-4497.
50. Zhou SY, Xie ZL, Xiao O, et al. Inhibition of mouse alkali burn induced-corneal neovascularization by recombinant adenovirus encoding human vasohibin-1. *Mol Vis*. 2010;26:16:1389-1398.
51. Suzuki Y, Kobayashi M, Miyashita H, et al. Isolation of a small vasohibin-binding protein (SVBP) and its role in vasohibin secretion. *J Cell Sci*. 2010;123:3094-3101.



## A scalable controlled-release device for transscleral drug delivery to the retina

Takeaki Kawashima<sup>a,1</sup>, Nobuhiro Nagai<sup>b,1</sup>, Hirokazu Kaji<sup>a,c</sup>, Norihiro Kumasaka<sup>b</sup>, Hideyuki Onami<sup>d</sup>, Yumi Ishikawa<sup>b</sup>, Noriko Osumi<sup>e</sup>, Matsuhiko Nishizawa<sup>a,c</sup>, Toshiaki Abe<sup>b,\*</sup>

<sup>a</sup> Department of Bioengineering and Robotics, Graduate School of Engineering, Tohoku University, 6-6-01 Aramaki-Aoba, Aoba-ku, Sendai 980-8579, Japan

<sup>b</sup> Division of Clinical Cell Therapy, Center for Advanced Medical Research and Development, ART, Tohoku University Graduate School of Medicine, 2-1 Seiryomachi, Aoba-ku, Sendai 980-8575, Japan

<sup>c</sup> JST, CREST, Sanbancho, Chiyoda-ku, Tokyo 102-0075, Japan

<sup>d</sup> Department of Ophthalmology, Tohoku University Graduate School of Medicine, 1-1 Seiryomachi, Aoba-ku, Sendai 980-8574, Japan

<sup>e</sup> Division of Developmental Neuroscience, Center for Neuroscience, ART, Tohoku University Graduate School of Medicine, 2-1 Seiryomachi, Aoba-ku, Sendai 980-8575, Japan

### ARTICLE INFO

#### Article history:

Received 13 October 2010

Accepted 3 November 2010

Available online 26 November 2010

#### Keywords:

Drug-delivery system

Transscleral delivery

Controlled release

Retinal neuroprotection

Polyethylene glycol

### ABSTRACT

A transscleral drug-delivery device, designed for the administration of protein-type drugs, that consists of a drug reservoir covered with a controlled-release membrane was manufactured and tested. The controlled-release membrane is made of photopolymerized polyethylene glycol dimethacrylate (PEGDM) that contains interconnected collagen microparticles (COLs), which are the routes for drug permeation. The results showed that the release of 40-kDa FITC-dextran (FD40) was dependent on the COL concentration, which indicated that FD40 travelled through the membrane-embedded COLs. Additionally, the sustained-release drug formulations, FD40-loaded COLs and FD40-loaded COLs pelletized with PEGDM, fine-tuned the release of FD40. Capsules filled with COLs that contained recombinant human brain-derived neurotrophic factor (rhBDNF) released bioactive rhBDNF in a manner dependent on the membrane COL concentration, as was found for FD40 release. When capsules were sutured onto sclerae of rabbit eyes, FD40 was found to spread to the retinal pigment epithelium. Implantation of the device was easy, and it did not damage the eye tissues. In conclusion, our capsule is easily modified to accommodate different release rates for protein-type drugs by altering the membrane COL composition and/or drug formulation and can be implanted and removed with minor surgery. The device thus has great potential as a conduit for continuous, controlled drug release.

© 2010 Elsevier Ltd. All rights reserved.

### 1. Introduction

The design of drug-delivery systems targeting the retina is a most challenging ophthalmological task. The principal delivery route currently in use is topical eye drop administration, but it delivers only low drug levels to the retina, and systemic drug delivery, e.g., intravenous delivery of Cytovene, a ganciclovir-type antiviral agent for cytomegalovirus [1], can produce toxic side effects. Although intravitreal delivery allows for high concentrations of a drug to be delivered directly to the retina, the necessary surgical procedure often requires repeated injections that can cause cataracts, retinal detachment, infection, and/or vitreous hemorrhage [2]. Therefore, transscleral delivery has emerged as a more attractive method for treating retinal disorders because it can deliver a drug locally and is less invasive [3,4]. Because of its large

surface area and high degree of hydration, the sclera is permeable to drugs of different sizes (up to ~70 kDa) [5]. Transscleral drug-delivery systems that range in size from microparticles to polymeric implants have been tested [6]. However, most of these systems are made of biodegradable polymers. Drug release profiles for biodegradable devices generally have a tri-phasic release profile, i.e., an initial burst, a diffusional release phase, and a final burst [7]. This complex profile occurs because the polymers erode with time and, by doing so, affect drug dissolution. Thus, a non-biodegradable device that contains a drug reservoir sealed with a semipermeable membrane allows for sustained release and reduces the sizes of the bursts [8].

Neuroprotection from retinal degenerative diseases by neurotrophic factor delivery to the retina remains a challenge for ophthalmology [9]. Intraocular administrations of brain-derived neurotrophic factor (BDNF) [10], ciliary neurotrophic factor [11], and basic fibroblast growth factor [12], have been shown to rescue degenerating photoreceptor cells in animals. Additionally, we have demonstrated that the implantation of genetically modified iris pigment epithelial cells that secrete BDNF to the subretinal space

\* Corresponding author. Tel./fax: +81 (0) 22 717 8234.

E-mail address: [toshi@oph.med.tohoku.ac.jp](mailto:toshi@oph.med.tohoku.ac.jp) (T. Abe).

<sup>1</sup> Equal contribution to this work.